LOCKHEED MARTIN ENERGY RESEARCH LIBRARIES
3 4456 0514204 8

CENTRAL RESEARCH LIBRARY
DOCUMENT COLLECTION

OAK RIDGE NATIONAL LABORATORY
operated by
UNION CARBIDE CORPORATION
NUCLEAR DIVISION
for the
U.S. ATOMIC ENERGY COMMISSION

ORNL-TM-3033
COPY NO. - 43
DATE - August 12, 1970

Neutron Physics Division

CALCULATION OF THE LONG-LIVED INDUCED ACTIVITY IN THE SOIL AROUND HIGH-ENERGY ACCELERATOR TARGET AREAS*

T. A. Gabriel

Abstract

Nucleon-meson cascade calculations have been carried out and estimates of the induced activity in the soil surrounding high-energy accelerator target areas have been obtained. Results on the contribution to the induced activity from various residual nuclei are presented for a specific irradiation time and as a function of time after beam shutdown for a 3-GeV proton accelerator.

OAK RIDGE NATIONAL LABORATORY
CENTRAL RESEARCH LIBRARY
DOCUMENT COLLECTION
LIBRARY LOAN COPY
DO NOT TRANSFER TO ANOTHER PERSON
If you wish someone else to see this
document, send in name with document
and the library will arrange a loan.

*Submitted for journal publication

NOTICE This document contains information of a preliminary nature and was prepared primarily for internal use at the Oak Ridge National Laboratory. It is subject to revision or correction and therefore does not represent a final report.

LEGAL NOTICE

This report was prepared as an account of Government sponsored work. Neither the United States, nor the Commission, nor any person acting on behalf of the Commission:

A. Makes any warranty or representation, expressed or implied, with respect to the accuracy, completeness, or usefulness of the information contained in this report, or that the use of any information, apparatus, method, or process disclosed in this report may not infringe privately owned rights; or

B. Assumes any liabilities with respect to the use of, or for damages resulting from the use of any information, apparatus, method, or process disclosed in this report.

As used in the above, "person acting on behalf of the Commission" includes any employee or contractor of the Commission, or employee of such contractor, to the extent that such employee or contractor of the Commission, or employee of such contractor prepares, disseminates, or provides access to, any information pursuant to his employment or contract with the Commission, or his employment with such contractor.

1. INTRODUCTION

The soil in the vicinity of high-energy accelerators, particularly around target areas, is continually bombarded with high-energy particles and becomes radioactive as a result of this bombardment. Since it is often necessary to remove this soil for either the construction of new facilities or the maintenance of existing facilities, it is desirable to have estimates of this activity. In this paper, calculated results are presented of the induced activity as a function of time in the concrete and surrounding soil of a beam target tunnel when 3-GeV protons are incident on a thick lead target in the tunnel.*

In Sec. 2 the calculational details are given. In Sec. 3 the results are presented and discussed.

*The calculations were carried out to aid in the design of the accelerator being constructed at the National Accelerator Laboratory.

LOCKHEED MARTIN ENERGY RESEARCH LIBRARIES

3 4456 0514204 8

2. CALCULATIONAL DETAILS

Shown in Fig. 1 is the geometry of the beam target tunnel. Cylindrical coordinates defined by ρ,z were used in all of the calculations. The Pb target is located at z = 0 and ρ = 0. The tunnel has a radius of 121.92 cm (4 ft) and is infinite in the positive and negative z directions. The concrete collar forming the tunnel has a thickness of 30.48 cm (1 ft). Outside the concrete is the soil which extends to infinity in the z and ρ directions. The concrete and soil composition used is shown in Table I[1]). The density of the concrete and soil was taken to be 2.36 g/cm^3 and 1.80 g/cm^3, respectively.

All the calculations presented here were carried out using the nucleon-meson transport code NMTC written by Coleman[2]), which allows for the transport of neutrons, protons, charged pions and muons, and takes into account elastic and nonelastic nuclear collisions, the continuous slowing down of charged particles, and the decay of pions and muons in flight. A detailed description of the code and its operation is given in[2]), and comparisons of results obtained with the code with experimental data are given in[2-4]). Calculations similar to those presented here have previously been carried out at somewhat lower energies by Gabriel[5]). The actual method of calculation used here is the same as that described in[5]). In the calculations the energy and angular distribution of the particles produced by 3-GeV proton-Pb nucleus collisions was taken from the intranuclear-cascade calculations of Bertini[6,7]). It was assumed that the Pb target was sufficiently thin that the attenuation of the particles in the target after they were produced could be neglected.

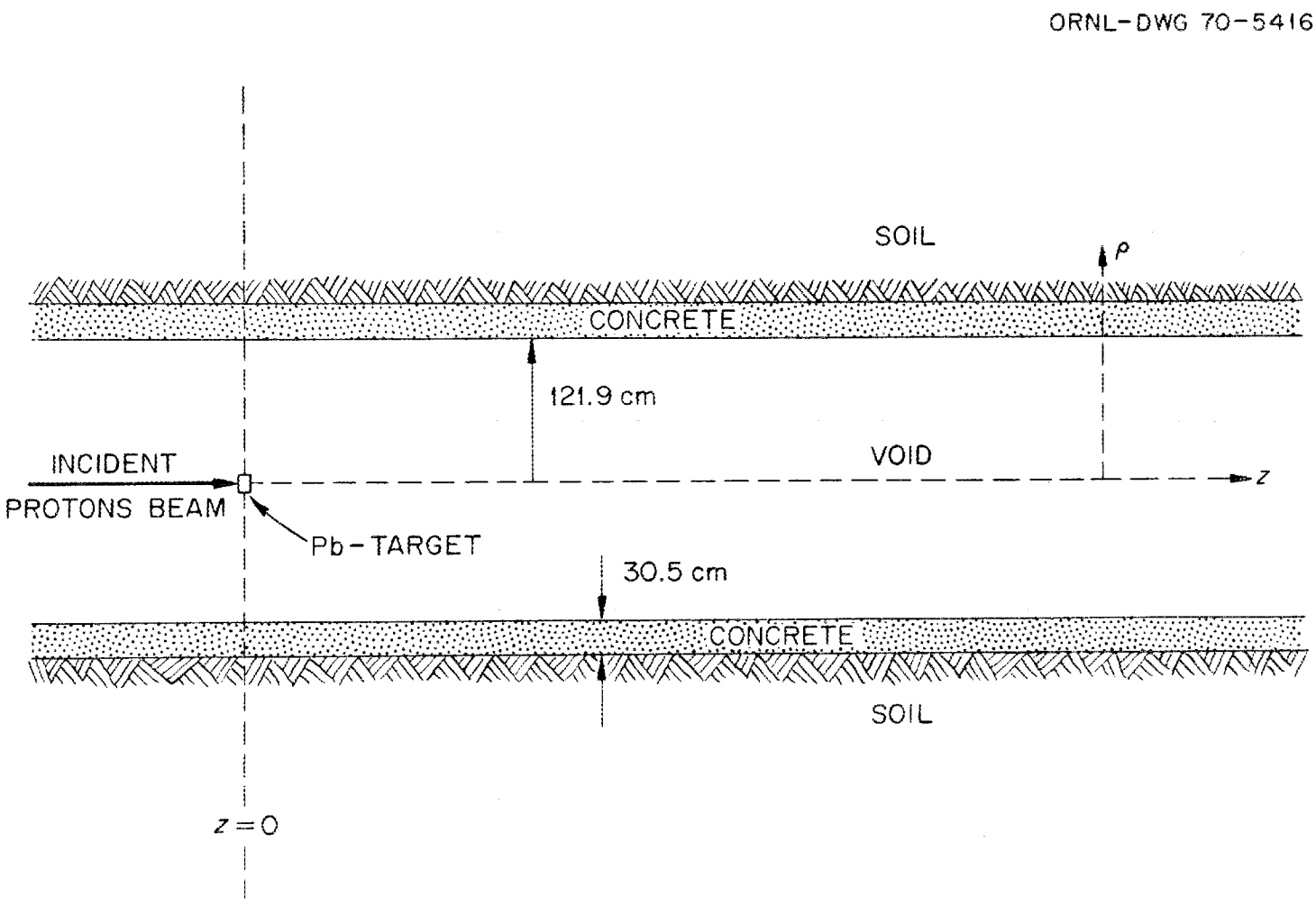

Fig. 1. Geometry and Variables of the Accelerator Target Tunnel.

TABLE I

Composition of Concrete and Soil

Element	Concrete (% by weight)	Soil (% by weight)
H	0.789	1.23
C	7.32	3.32
O	51.54	55.03
Na	0.063	0.396
Mg	6.54	2.09
Al	0.456	5.51
Si	10.19	22.85
S	0.158	0
K	0.071	0.517
Ca	21.09	6.08
Fe	1.61	2.91

If the neutron, proton, and pion fluxes are known, the induced activity in the soil and in the concrete may be calculated from the expression

$$A(\rho,z,t_i,t_s,I) = \sum_k A_k(\rho,z,t_i,t_s,I) = \sum_k P_k(\rho,z)(1 - e^{-\lambda_k t_i}) e^{-\lambda_k t_s} \tag{1}$$

$$P_k(\rho,z) = \sum_i \sum_j I \int_{E_{th_{kji}}}^{E_{max}} dE_i \; \eta_j \; \sigma_{ijk}(E_i) \; \Phi_i(\rho,z,E_i) \; ,$$

where

$A(\rho,z,t_i,t_s,I)$ = the total activity at ρ,z for an irradiation time of t_i and a time after shutdown of t_s when there are I 3-GeV proton-Pb nucleus collisions/sec;

$A_k(\rho,z,t_i,t_s,I)$ = the partial activity of the kth-type of radioactive nucleus;

$P_k(\rho,z)$ = the production rate of the kth-type radioactive nucleus for one proton-Pb nucleus collision in the target;

λ_k = the decay rate of the kth-type nucleus;

$E_{th_{kji}}$ = the threshold energy for producing the kth-type nuclei from a nucleus of type j by a particle of type i;

η_j = the number of density nuclei of type j;

$\sigma_{ijk}(E_i)$ = the microscopic cross section for the production of a nucleus of type k when a particle of type i collides with a target nucleus of type j;

$\Phi_i(\rho,z,E_i)$ = the omnidirectional flux per unit energy of particles of type i due to one proton-Pb nucleus collision in the target.

The activity in the soil and concrete was calculated from Eq. 1 using only proton and neutron fluxes. The pion fluxes were calculated, and it was determined that they were sufficiently small compared to the nucleon fluxes that the activity induced by pions could be neglected. The cross-section data used in calculating the activity are taken from[5-17]). All radioactive nuclei which can be produced from the elements in the concrete and soil and which have half-lives greater than one day were considered. A list of these nuclei, along with their half-lives, is given in Table II. It should be noted that several nuclei (see Table II) which have half-lives less than one day can decay into long-lived nuclei ($\tau_{1/2}$ > 1 day). The production of these nuclei was also considered. It was assumed that these shorter lived nuclei when produced decayed instantly into the longer lived nuclei. Some of the long-lived nuclei decay into nonstable elements. In calculating the induced activity produced by these nuclei, the subsequent secondary decays have not been included. Some of the listed nuclei, indicated by *, have two decay rates. Because of the method in which some of the production cross sections for these elements were calculated[5,9]), it was not possible to distinguish between the isomeric states formed. It was therefore assumed that the cross sections obtained represented the isomeric state which has the greater half-life.

3. RESULTS AND DISCUSSION

The results of the calculations are presented in Figs. 2 and 3 and in Table III. All of the results are given assuming 10^{13} 3-GeV proton-Pb nucleus collisions/sec. In Fig. 2 the total induced activity as a function of spatial position for an irradiation time of 25 years and a time after shutdown of 1 month is shown. The top curve represents the activity in the

TABLE II

Radioactive Nuclei ($z < 28$) with Half-Lives > 1 Day

Element	Half-Life (years)	
^{3}H	1.23×10^{1}	
^{7}Be	1.47×10^{-1}	
^{10}Be	2.70×10^{6}	
^{14}C	5.77×10^{3}	
^{22}Na	2.58×10^{0}	
* ^{26}Al	7.40×10^{5}	$(^{26}Si \xrightarrow{2\ sec} {}^{26}Al + \beta^{+})$
^{32}Si	7.00×10^{2}	$^{32}Si \longrightarrow {}^{32}P + \beta^{-}$
^{32}P	3.92×10^{-2}	
^{33}P	6.85×10^{-2}	
^{35}S	2.37×10^{-1}	
^{36}Cl	3.00×10^{5}	
^{37}Ar	9.39×10^{-2}	$(^{37}K \xrightarrow{1.2\ sec} {}^{37}Ar + \beta^{+})$
^{39}Ar	2.60×10^{2}	$(^{39}Cl \xrightarrow{55.5\ min} {}^{39}Ar + \beta^{-})$
^{42}Ar	3.30×10^{1}	$^{42}Ar \longrightarrow {}^{42}K + \beta^{-} \xrightarrow{12.4\ h} {}^{42}Ca + 2\beta^{-}$
^{40}K	1.30×10^{9}	
^{41}Ca	1.10×10^{5}	$(^{41}S \xrightarrow{0.87\ sec} {}^{41}Ca + \beta^{+})$
^{45}Ca	4.52×10^{-1}	$(^{45}K \xrightarrow{20\ min} {}^{45}Ca + \beta^{-})$
^{47}Ca	1.29×10^{-2}	$^{47}Ca \longrightarrow {}^{47}Sc + \beta^{-}$
* ^{44}Sc	6.57×10^{-3}	
* ^{46}Sc	2.30×10^{-1}	
^{47}Sc	9.31×10^{-3}	$^{44}Ti + e^{-} \longrightarrow {}^{44}Sc$
^{48}Sc	5.02×10^{-3}	
^{44}Ti	4.70×10^{1}	
^{48}V	4.41×10^{-2}	$(^{48}Cr + e^{-} \xrightarrow{23\ h} {}^{48}V)$
^{49}V	9.04×10^{-1}	$(^{49}Cr \xrightarrow{42\ min} {}^{49}V + \beta^{+})$
^{51}Cr	7.61×10^{-2}	$(^{51}Mn \xrightarrow{45\ min} {}^{51}Cr + \beta^{+})$
* ^{52}Mn	1.53×10^{-2}	$(^{52}Fe \xrightarrow{8\ h} {}^{52}Mn + \beta^{+})$
^{53}Mn	2.00×10^{6}	$(^{53}Fe \xrightarrow{9\ min} {}^{53}Mn + \beta^{+})$
^{54}Mn	7.97×10^{-1}	
^{55}Fe	2.70×10^{0}	$(^{55}Co \xrightarrow{18\ h} {}^{55}Fe + \beta^{+})$
^{59}Fe	1.23×10^{-1}	
^{56}Co	2.19×10^{-1}	
^{57}Co	7.31×10^{-1}	
* ^{58}Co	1.97×10^{-1}	

*Indicates elements that have two decay rates.

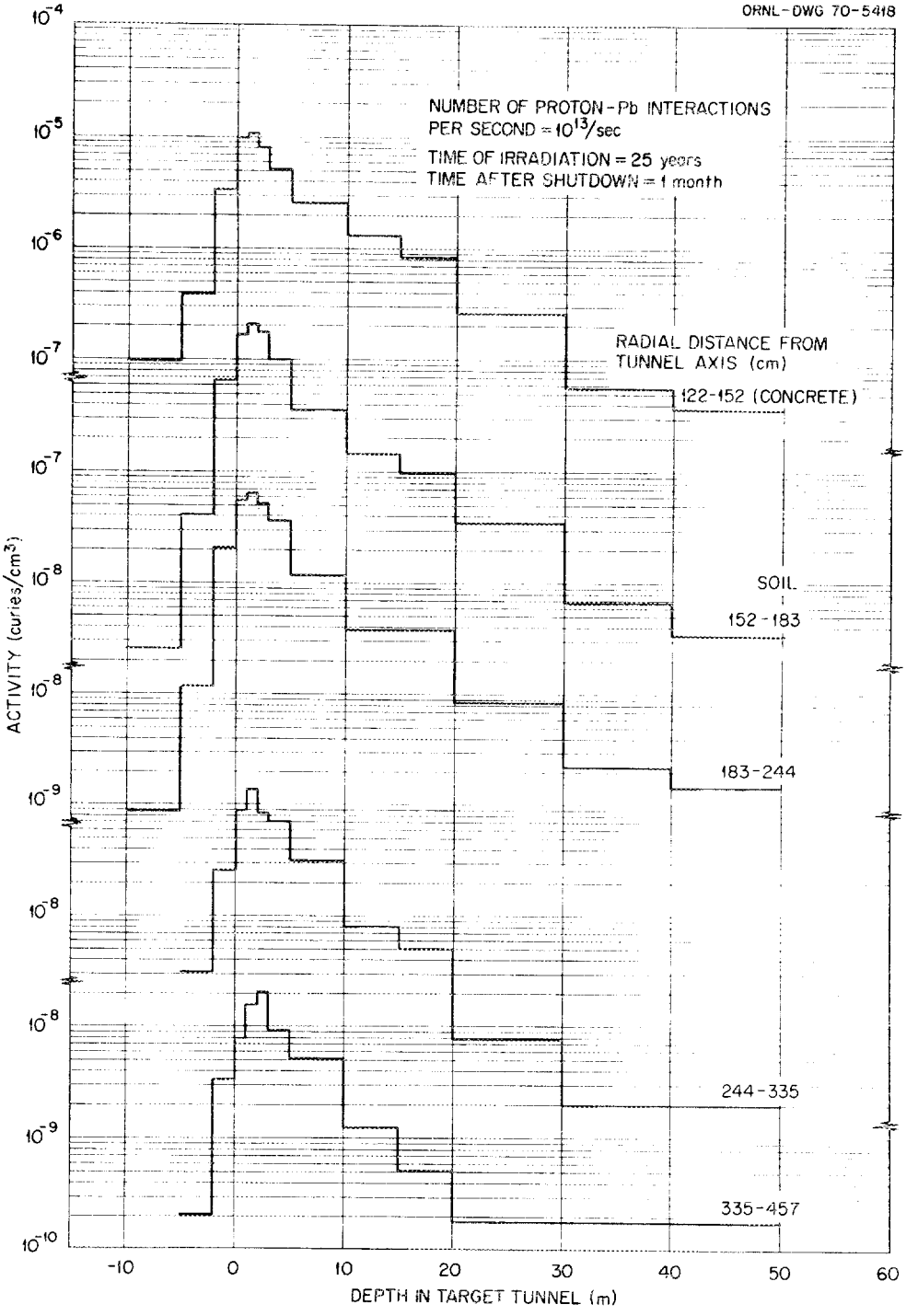

Fig. 2. Spatial Dependence of the Total Induced Activity.

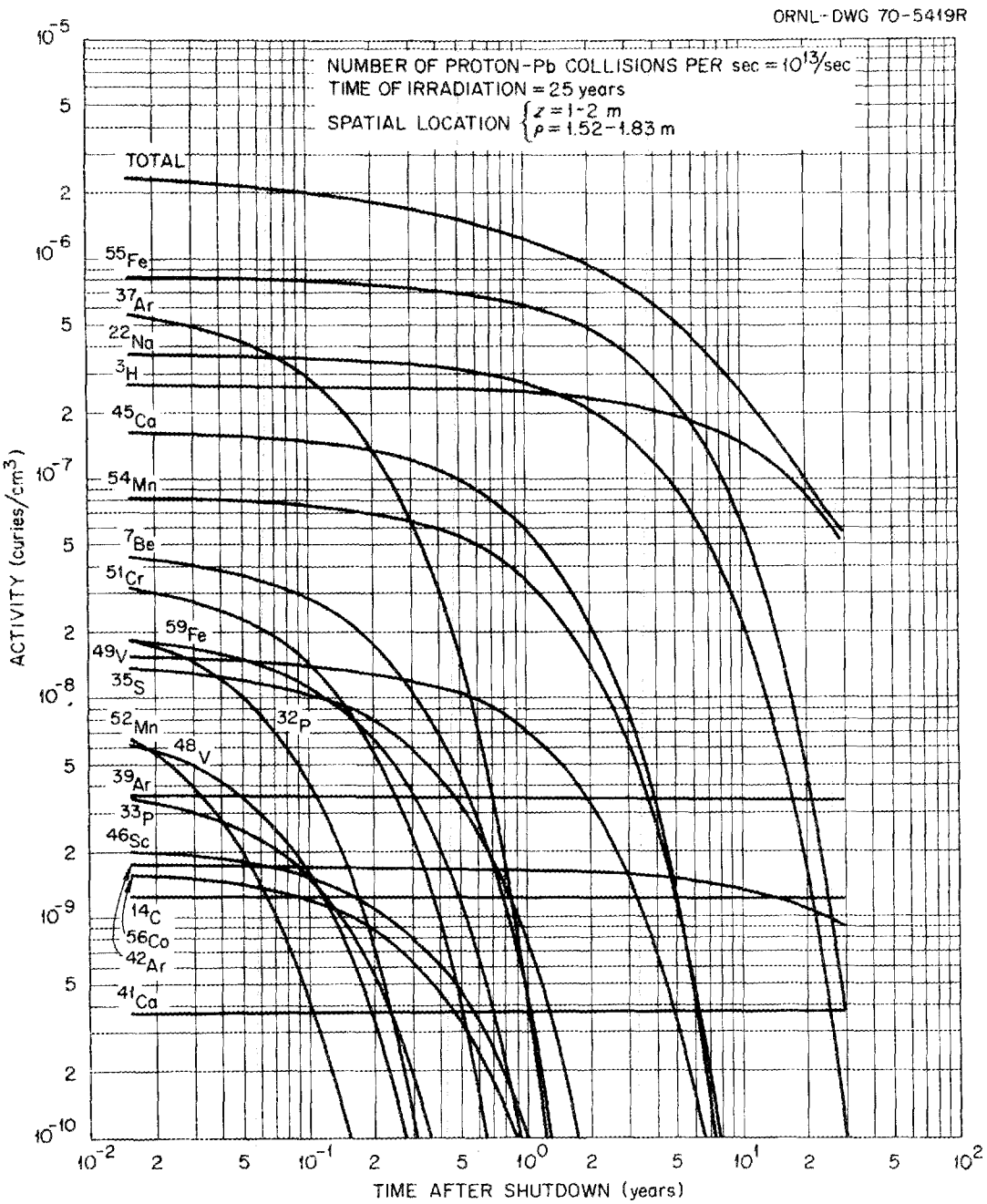

Fig. 3. Time Dependence of the Total Induced Activity Showing Selected Individual Contributions.

TABLE III

Activity Due to Individual Nuclides Averaged Over the Interval z = 1 m to z = 2 m and Over the Indicated Radial Intervals

	Number of 3-GeV Proton-Pb Nucleon Collisions/sec = 10^{13}/sec				
	Time of Irradiation = 25 years Time After Shutdown = 1 month				
	Activity (Ci/cm^3)				
Element	ρ = 122 to 152 cm	ρ = 152 to 183 cm	ρ = 183 to 244 cm	ρ = 244 to 335 cm	ρ = 335 to 457 cm
^{3}H	1.56×10^{-6}	2.61×10^{-7}	8.41×10^{-8}	1.67×10^{-8}	1.70×10^{-9}
^{7}Be	2.51×10^{-7}	3.11×10^{-8}	9.35×10^{-9}	1.80×10^{-9}	1.68×10^{-10}
^{10}Be	1.93×10^{-12}	2.96×10^{-13}	1.06×10^{-13}	2.18×10^{-14}	2.67×10^{-15}
^{14}C	4.13×10^{-9}	1.27×10^{-9}	4.44×10^{-10}	9.64×10^{-11}	1.16×10^{-11}
^{22}Na	1.49×10^{-6}	3.56×10^{-7}	1.30×10^{-7}	2.77×10^{-8}	3.32×10^{-9}
^{26}Al	4.05×10^{-11}	3.16×10^{-11}	1.11×10^{-11}	2.35×10^{-12}	2.77×10^{-13}
^{32}Si	4.67×10^{-11}	2.46×10^{-12}	8.56×10^{-13}	1.93×10^{-13}	2.04×10^{-14}
^{32}P	7.88×10^{-8}	5.59×10^{-9}	2.02×10^{-9}	4.13×10^{-10}	4.84×10^{-11}
^{33}P	2.05×10^{-8}	1.78×10^{-9}	6.48×10^{-10}	1.41×10^{-10}	1.58×10^{-11}
^{35}S	1.34×10^{-7}	1.11×10^{-8}	4.07×10^{-9}	8.90×10^{-10}	9.95×10^{-11}
^{36}Cl	7.15×10^{-11}	6.90×10^{-12}	2.47×10^{-12}	5.35×10^{-13}	6.19×10^{-14}
^{37}Ar	4.33×10^{-6}	3.30×10^{-7}	1.06×10^{-7}	2.64×10^{-8}	2.90×10^{-9}
^{39}Ar	2.46×10^{-8}	3.70×10^{-9}	1.21×10^{-9}	2.72×10^{-10}	2.83×10^{-11}
^{42}Ar	2.13×10^{-8}	1.68×10^{-9}	6.07×10^{-10}	1.32×10^{-10}	1.70×10^{-11}
^{40}K	1.04×10^{-13}	3.13×10^{-14}	8.94×10^{-15}	1.84×10^{-15}	2.22×10^{-16}
^{41}Ca	3.20×10^{-5}	3.73×10^{-10}	1.03×10^{-10}	1.98×10^{-11}	2.54×10^{-12}
^{45}Ca	1.21×10^{-6}	1.44×10^{-7}	3.97×10^{-8}	7.60×10^{-9}	9.78×10^{-10}
^{47}Ca	1.77×10^{-10}	1.75×10^{-11}	5.81×10^{-12}	1.10×10^{-12}	1.23×10^{-13}
^{44}Sc	1.25×10^{-12}	4.36×10^{-13}	1.49×10^{-13}	3.24×10^{-14}	3.50×10^{-15}
^{46}Sc	4.11×10^{-9}	1.58×10^{-9}	5.47×10^{-10}	1.26×10^{-10}	1.40×10^{-11}
^{47}Sc	5.69×10^{-12}	2.24×10^{-12}	7.68×10^{-13}	1.93×10^{-13}	1.99×10^{-14}
^{48}Sc	1.15×10^{-14}	3.02×10^{-15}	9.30×10^{-16}	2.09×10^{-16}	1.85×10^{-17}
^{44}Ti	1.32×10^{-10}	3.78×10^{-11}	1.22×10^{-11}	2.22×10^{-12}	2.32×10^{-13}
^{48}V	4.97×10^{-9}	2.14×10^{-9}	7.87×10^{-10}	2.03×10^{-10}	1.99×10^{-11}
^{49}V	3.41×10^{-8}	1.46×10^{-8}	5.18×10^{-9}	1.12×10^{-9}	1.27×10^{-10}
^{51}Cr	3.53×10^{-8}	1.70×10^{-8}	6.14×10^{-9}	1.34×10^{-9}	1.43×10^{-10}
^{52}Mn	1.40×10^{-9}	6.72×10^{-10}	2.45×10^{-10}	5.29×10^{-11}	6.11×10^{-12}
^{53}Mn	1.86×10^{-12}	9.20×10^{-13}	3.31×10^{-13}	7.02×10^{-14}	9.24×10^{-15}
^{54}Mn	1.59×10^{-7}	7.76×10^{-8}	2.77×10^{-8}	6.06×10^{-9}	7.44×10^{-10}
^{55}Fe	1.12×10^{-6}	7.84×10^{-7}	2.26×10^{-7}	4.28×10^{-8}	5.26×10^{-9}
^{59}Fe	1.25×10^{-8}	9.36×10^{-9}	2.58×10^{-9}	4.91×10^{-10}	6.33×10^{-11}
^{56}Co	5.60×10^{-9}	1.27×10^{-9}	3.69×10^{-10}	1.30×10^{-10}	2.60×10^{-14}
^{57}Co	1.52×10^{-10}	3.43×10^{-11}	9.98×10^{-12}	3.51×10^{-12}	8.06×10^{-16}
^{58}Co	1.79×10^{-11}	4.06×10^{-12}	1.18×10^{-12}	4.16×10^{-13}	8.33×10^{-17}
TOTAL	1.05×10^{-5}	2.05×10^{-6}	6.47×10^{-7}	1.34×10^{-7}	1.57×10^{-8}

concrete and the remaining four curves represent the activity in the soil. The radial intervals over which the activity has been averaged are specified in the figure. The statistical errors associated with the histograms in Fig. 2 are estimated to be < 10% when the activity is > 5×10^{-6} Ci/cm^3 and to increase by 10-15% with each order of magnitude decrease in the activity.

In Table III the contributions to the activity of each of the 34 nuclides averaged over the interval z = 1 m to z = 2 m and over several radial intervals are given. The statistical errors associated with the entries in Table III are < 10% for the first column, < 15% for the second column, < 20% for the third column, < 30% for the fourth column, and < 45% for the fifth column. If it is assumed that the relative contribution of each nuclide to the total activity is independent of position, then curves analogous to those in Fig. 2 for each nuclide may be obtained by renormalizing the curves in Fig. 2 in accordance with the values for each nuclide given in Table III. The curves obtained in this manner are, of course, only approximate, but for nuclides that have relatively low threshold-production values ($\gtrsim$ 50 MeV), the approximation is fair - of the order of 30% at the extremes of the z dependence (z = -10 m and z = 50 m), shown in Fig. 2. The approximation is less valid for the nuclides which have higher threshold production values, and the error for these nuclides can approach 500% for z of the order of -10 m and 200% for z of the order of 50 m.

In Fig. 3 the total induced activity averaged over the intervals z = 1 m to z = 2 m and ρ = 152 cm to 183 cm and the activity due to several nuclides averaged over the same spatial region are shown as a function of time after shutdown. The individual nuclides shown in the figure are those that contribute the most to the total activity. The relative importance of the

various nuclides in Fig. 3 is approximately the same as that found in the lower energy case considered in[5]).

ACKNOWLEDGMENTS

The many helpful discussions with Dr. R. G. Alsmiller, Jr. and Dr. T. W. Armstrong are gratefully acknowledged and appreciated.

REFERENCES

[1] M. Awschalom *et al.*, "Chemical Composition of Some Common Shielding Materials," National Accelerator Laboratory Report TM-168 (0160) (1969).

[2] W. A. Coleman and R. G. Alsmiller, Jr., Nucl. Sci. Eng. 34, 104 (1968).

[3] T. W. Armstrong and R. G. Alsmiller, Jr., Nucl. Sci. Eng. 33, 291 (1968).

[4] T. W. Armstrong, J. Geophys. Res. 74, 1361 (1969).

[5] T. A. Gabriel, "Calculation of the Long-Lived Induced Activity in Soil Produced by 200-MeV Protons," ORNL-TM-2848 (1970).

[6] H. W. Bertini, "Preliminary Data from Intranuclear-Cascade Calculations of 0.75-, 1-, and 2-GeV Protons on Oxygen, Aluminum, and Lead, and 1-GeV Neutrons on the Same Elements," ORNL-TM-1996 (1967).

[7] H. W. Bertini *et al.*, "Intranuclear-Cascade Calculation of Secondary Nucleon Spectra from Nucleon-Nucleus Interactions in the Energy Range 340 to 2900 MeV and Comparison with Experiment," ORNL-TM-2361 (1969).

[8] H. W. Bertini *et al.*, "Literature Survey of Radiochemical Cross-Section Data Below 425 MeV," ORNL-3884 (1966).

[9] H. W. Bertini, "Comparison of Calculated Radiochemical Cross Sections with Experimental Results for Incident Protons and π^- Mesons in the 50- to 400-MeV Region: Effect of Varying a Few Nuclear Parameters in the Calculations," ORNL-4105 (1968).

[10] W. Edward Alley *et al.*, "Semiempirical Neutron-Induced Reaction Cross Sections," Lawrence Radiation Laboratory Report UCRL-50484 (1968).

[11] S. G. Rudstam, Z. Naturforsch. 21a, 1027 (1966), and Nucl. Phys. A126, 401 (1969).

[12] R. Bernas *et al.*, Ann. Phys. 44, 426 (1967).

13) F. Yiou *et al.*, J. Geophys. Res., Space Phys., 74, 2447 (1969).

14) E. L. Fireman and F. S. Rowland, Phys. Rev. 97, 780 (1955).

15) G. Friedlander *et al.*, Phys. Rev. 99, 263 (1955).

16) M. Honda and D. Lal, Nucl. Phys. 51, 363 (1964).

17) E. Baker *et al.*, Phys. Rev. 112, 1319 (1958).

Internal Distribution

1-3. L. S. Abbott
4. F. S. Alsmiller
5. R. G. Alsmiller, Jr.
6. T. W. Armstrong
7. H. W. Bertini
8. C. E. Clifford
9-33. T. A. Gabriel
34. M. P. Guthrie
35. W. E. Kinney
36. T. A. Love
37. F. C. Maienschein
38. R. W. Peelle
39. R. W. Roussin
40. R. T. Santoro
41. D. Sundberg
42. D. K. Trubey
43. J. W. Wachter
44. H. A. Wright
45. W. Zobel
46. E. R. Cohen (consultant)
47. H. Feshbach (consultant)
48. H. Goldstein (consultant)
49-50. Central Research Library
51. ORNL Y-12 Technical Library, Document Reference Section
52-53. Laboratory Records Department
54. Laboratory Records ORNL RC
55. ORNL Patent Office

External Distribution

56. P. B. Hemmig, Division of Reactor Development & Technology, U. S. Atomic Energy Commission, Washington, D. C.
57. W. H. Hannum, Division of Reactor Development & Technology, U. S. Atomic Energy Commission, Washington, D. C.
58. Kermit Laughon, AEC Site Representative.
59-155. Given AEC High-Energy Accelerator Shielding Distribution*

156-169. Division of Technical Information (DTIE).
170. Laboratory and University Division (ORO).

*This distribution list is available upon request.